EC Stray Detection system Planning 2021/2022

A. Moro, L. Figini (ISTP - CNR)
C. Piccinni (IPP - Garching)

This work has been carried out within the framework of the EUROfusion Consortium and has received funding from the European Union's Horizon 2020 research and innovation programme under grant agreement number 633053.

Outline

- Return of experience from previous analysis
- Choice for ECH sensor (the ITER option)
- Estimated load on the vessel with EC configuration for first plasma
- Proposed planning for 2021/2022 activities

Return of experience from previous analysis

In WPSA the EC stray radiation issue for JT-60SA has been studied:

1. EC Stray radiation modelling in JT-60SA during operations (A. Moro et al., Deliverable 2016)
2. ECR stray Radiation Loads on the Cryopumps of JT-60SA (M. Wanner, Tech. Note 2019)
3. Evaluation of the ECRF stray radiation power (C. Sozzi et al., Deliverable 2019)

- Qualitative and quantitative evaluation of P_{den} due to residual non-absorbed EC power fraction considering **low absorption scenarios**, **specific in vessel locations**, and including **launching angles, EC modes** and **plasma temperature** dependences.
- General outcome: **reference values** and **guidelines** as starting point for safety purposes.

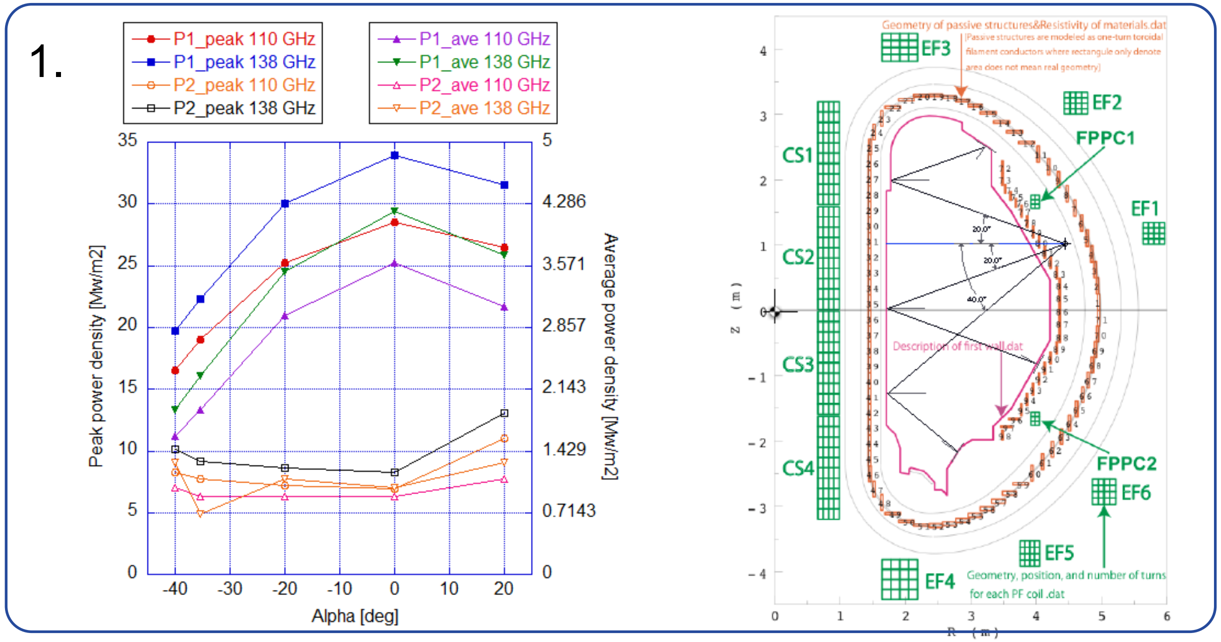

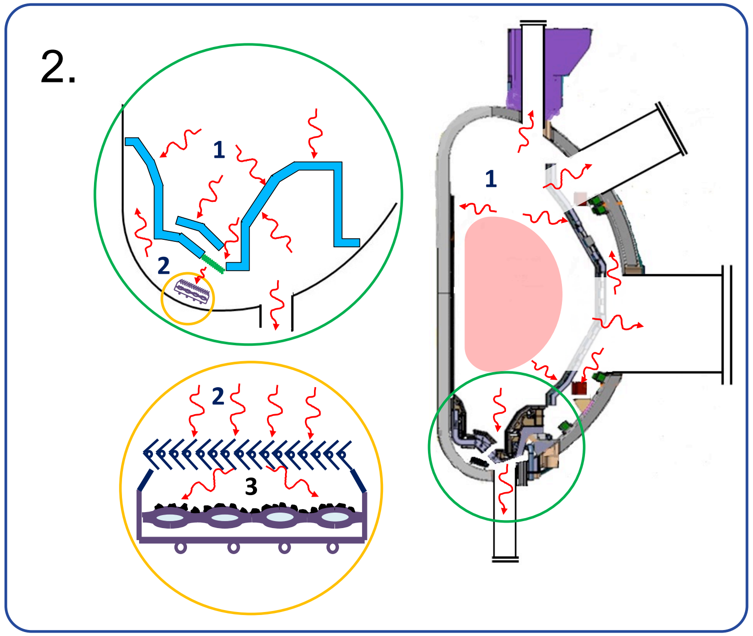

Return of experience from previous analysis

Gaussian beam propagation, coupled resonators model, beam tracing and PO codes

3.

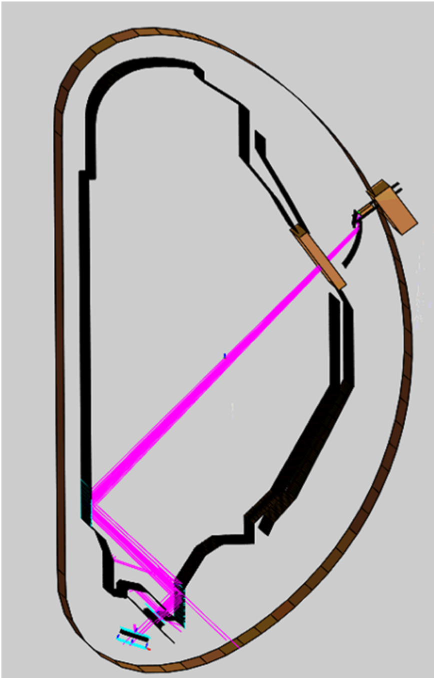

Simplified representation stabilizing plate and the sub-divertor region (cryopumps location).

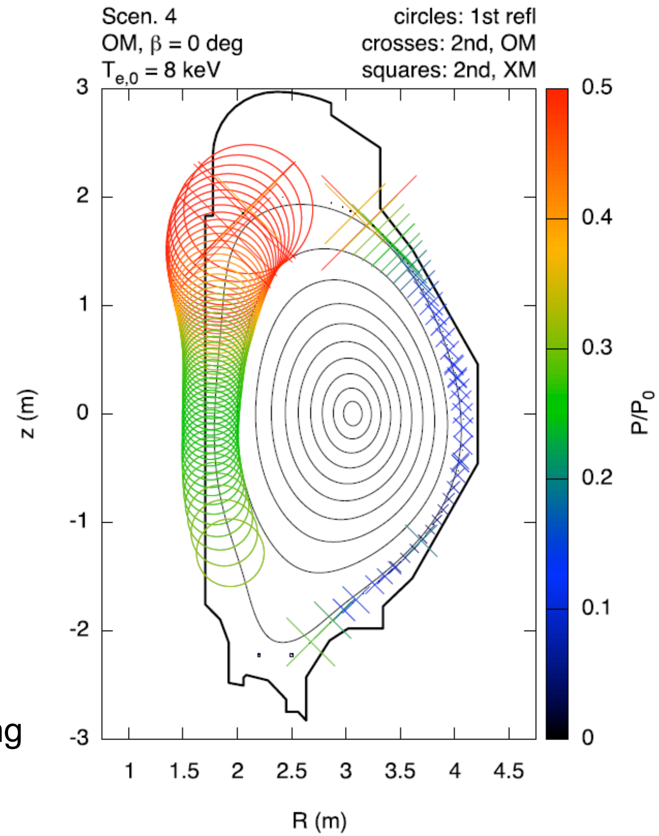

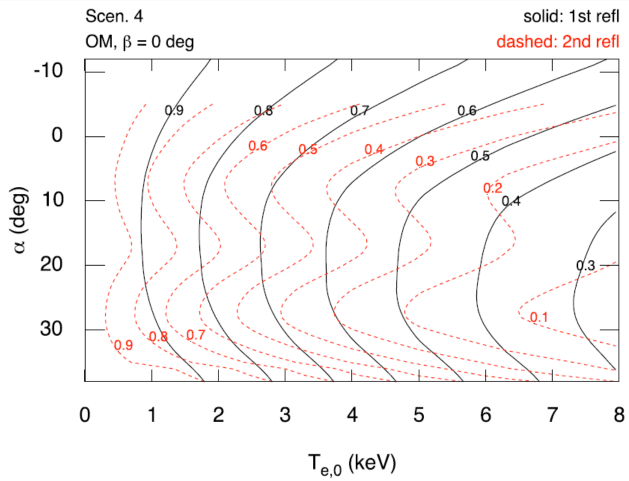

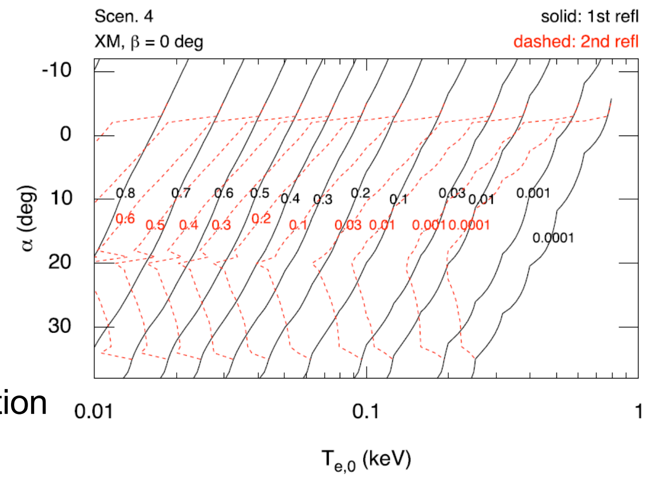

GRAY simulation of residual EC distribution and with T_e down-scaling.

EC injection in a condition of zero (pre-ionization and ECWC experiments) or very low fraction of absorbed power ~0.1 (assisted burn-through experiments) results in $P \geq 0.9\ P_0$ hitting the inner wall at the first pass, with **several MW/m²** per injected beam.

Return of experience from previous analysis

Distribution of the non-absorbed EC power fraction after 1 and 2 passes was calculated considering:

- a small fraction (5%) of (wrong) OM2 polarization
- main XM2 component, with higher absorption, in low T_e conditions

Residual cross polarized fraction (5%) at 5 keV plasma temperature

(kW/m² per 1MW injected beam)	peak incident power density (scen 2)		estimated peak absorbed power density on CFC (scen 2)		peak incident power density (scen 4)		estimated peak absorbed power density on CFC (scen 4)		duration
poloidal angle	1st bounce	2nd bounce	1st bounce	2nd bounce	1st bounce	2nd bounce	1st bounce	2nd bounce	
0	508.50	18.68	45.26	1.66	1017.00	99.60	90.51	8.86	pulse length
-20	375.00	10.75	33.38	0.96	70.50	6.06	6.27	0.54	
-35.5	334.50	41.40	29.77	3.68	61.33	13.41	5.46	1.19	

Low absorption scenario at low plasma temperature (50 eV)

(kW/m² per 1MW injected beam)	peak incident power density (scen 2)		estimated peak absorbed power density on CFC (scen 2)		peak incident power density (scen 4)		estimated peak absorbed power density on CFC (scen 4)		duration
poloidal angle	1st bounce	2nd bounce	1st bounce	2nd bounce	1st bounce	2nd bounce	1st bounce	2nd bounce	
0	6780.00	16.60	603.42	1.48	16950.00	1660.00	1508.55	147.74	1-1000 ms
-20	3000.00	8.60	267.00	0.77	9000.00	180.60	801.00	16.07	
-35.5	669.00	0.28	59.54	0.02	3345.00	276.00	297.71	24.56	

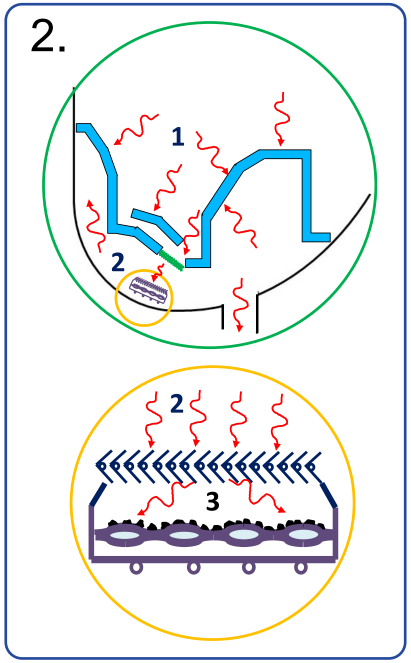

P_{stray}=150 kW*, water baffle uncoated; α = 0.04

Power flux	kW/m²	Absorbed power	W
- Volume 1	5.783	Water baffle	168
- Volume 2	0.400	Cryopump 80 K baffle	3114
- Volume 3	0.115	Cryopump panel	41

P_{stray}=150 kW,* water baffle coated; α = 0.7

Power flux	kW/m²	Absorbed power	W
- Volume 1	5.774	Water baffle	2809
- Volume 2	0.125	Cryopump 80 K baffle	972
- Volume 3	0.036	Cryopump panel	13

*Assuming:

- XM2 injection, 95% absorption
- residual 5% OM2 (coupled resonator approach),
- isotropic stray distribution

- The radiation fluxes may reach significant levels (even larger with tungsten),
- Baffles overloaded, coating recommended (Al_2O_3 and TiO_2)

Choice for ECH sensor (the ITER option)

The principle of differential thermocouple configuration allows to **separate the microwave and neutrons loads**, measuring P_{den} as low as 0.5 kW/m^2 up to 1.25 MW/m^2 in steady state and transients up to 3 MW/m^2 for 5.5 s

$$\Delta V = (S_A - S_C)(T_2 - T_1)$$

$$\alpha_{1,2} p_\mu S = \rho c V \frac{d\Delta T}{dt} + U_{eq}\Delta T$$

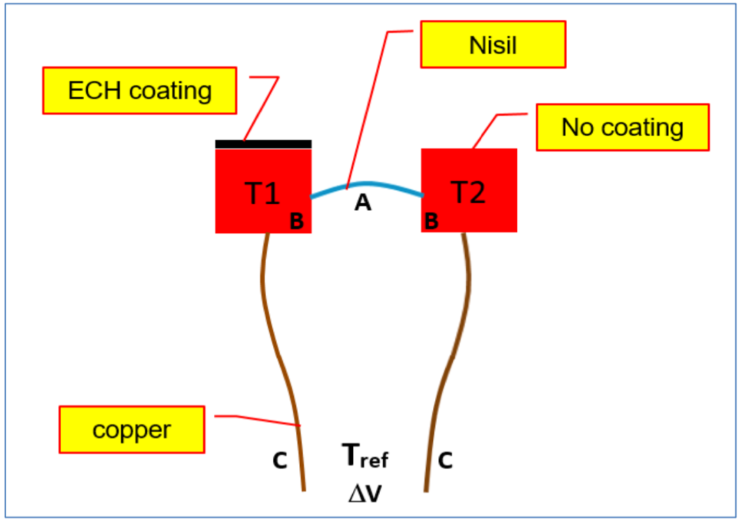

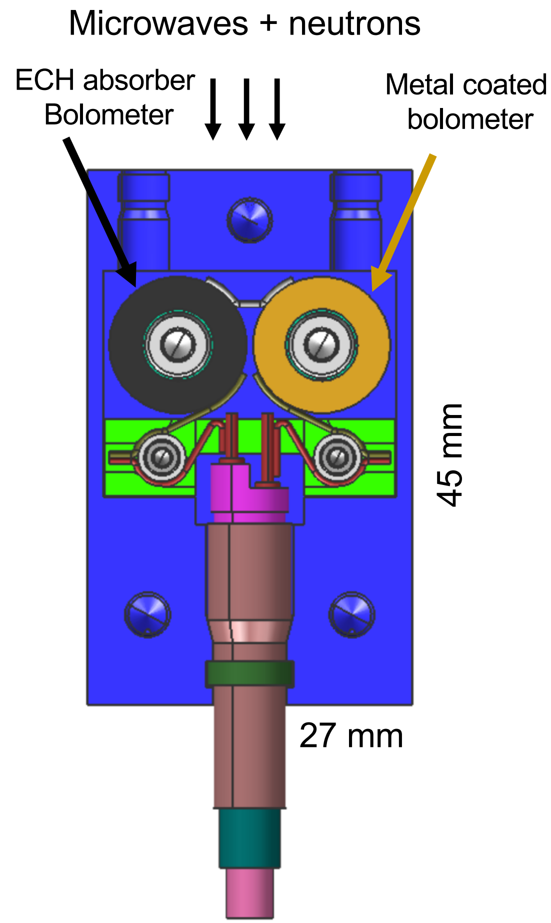

Specification	Symbol	Value
Sensor volume [mm^3]	V	45x27x13 mm^3
Internal thermal conductivity	k_{int}	390 W/mK
Difference in Seebeck coefficients	S_{Cr}-S_{Al}	41 mV/℃
Temperature range	ΔT	[100-816 ℃]
Transient sensitivity in temperature	dΔT/dt/p	1.93 10^{-5} K m^2/J
Steady state sensitivity in temperature	dΔT/dt/p	5.65 10^{-4} K m^2/J
Response time	t	1.3 s

Extensive design studies, prototyping and tests

N. Masseen et al., "Microwave Detector design for ITER", ITER_D_JR2KH6

A. Sirinelli, "System Design Description (DDD) 55.GB In-vessel ECH Detectors", ITER_D_V2GEA7 v1.0

A. Sirinelli, "55.GB – Return of experience Report", ITER_D_UYRF93

Choice for ECH sensor (the ITER option)

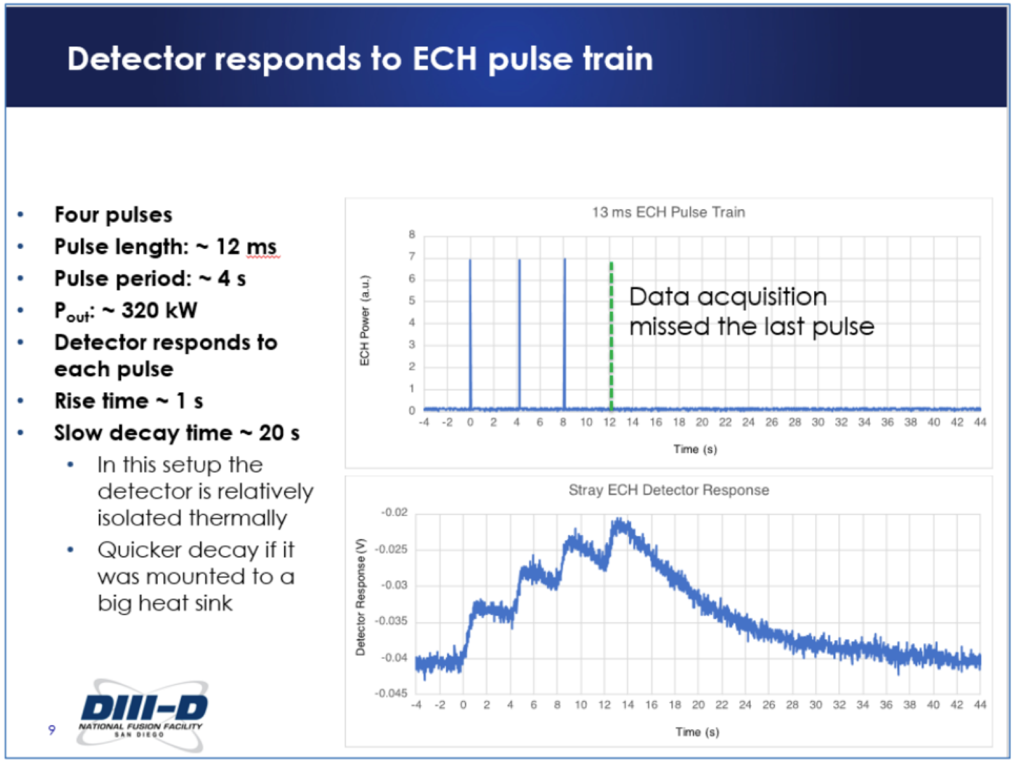

Detector response to ECH pulses at DIII-D (2018).

A. Sirinelli "55.GB – Return of experience Report", ITER_D_UYRF93

The principle of differential thermocouple arrangement works

Additional possibility is to develop a system combining the differential thermocouples bolometer with

- pyrodetectors: proved to be fast and sensitive as safety system (not ok for mm-wave diagnostic, large n flux, long pulse signal drift are open issues)
- sniffer probes (oversized waveguides), see W-7X (S. Marsen et al., https://doi.org/10.1088/1741-4326/aa6ab2)
- graphene bolometers?

Response time 10^2–10^3 μs
Aperture $\sim$5 mm^2 , FOV >75°
Thermal time constant $\tau \sim$ 150 ms

A. Moro et al
https://doi.org/10.1016/j.fusengdes.2017.03.028

Estimated EC load on the vessel (1st plasma)

Antenna parameters for 1st plasma	
Beam waist radius w_0 [mm]	19.42
Launching point coordinates (R,Z) [mm]	(5214.0, 1722.0)
Poloidal injection angle a [deg]	-35.5

- Divergent gaussian beam
- Lower loads on ‘empty’ vessel wrt final antenna configuration

Incident power density (MW/m^2 per 1 MW injected beam)				
Frequency [GHz]	1st bounce (@ R=1.708 m, Z= -0.733 m, θ=35.5 deg)		2nd bounce (@ R=3.661 m, Z=-2.123 m, θ=8.86 deg)	
	$P_{dens}(0,z)$	$P_{av}(z)$	$P_{dens}(0,z)$	$P_{av}(z)$
82	7.702	0.963	3.852	0.482
110	13.8	1.725	6.92	0.865
138	21.59	2.699	10.86	1.358

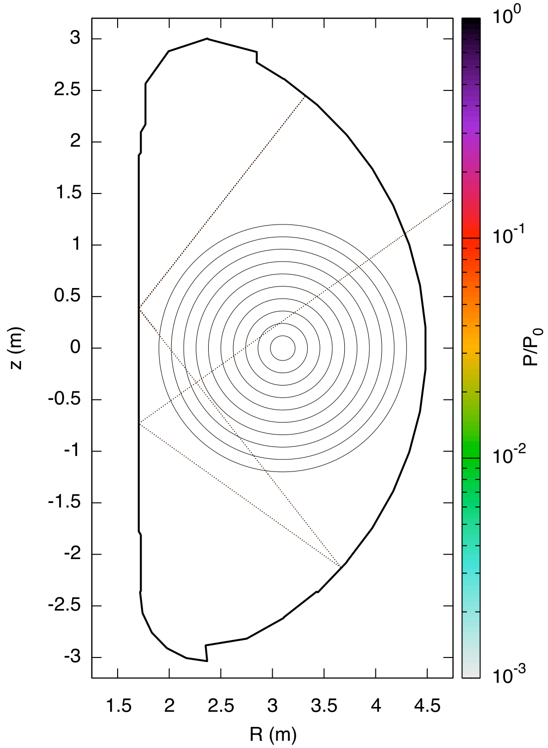

Incident power density at first bounce (MW/m^2 per 1 MW injected beam)				
Frequency [GHz]	n [10^{19} m^{-3}]	T [keV]	$P_{dens}(0,z)$	$P_{av}(z)$
82	0.01	0.1	7.69	0.96
	0.1	0.3	7.32	0.91
	1.0	1.0	2.37	0.30
110	0.01	0.1	13.74	1.72
	0.1	0.3	11.72	1.46
	1.0	1.0	0.07	0.01
138	0.01	0.1	21.49	2.69
	0.1	0.3	18.48	2.31
	1.0	1.0	0.14	0.02

- Circular plasma, R_{ax} = 3.1 m, z_{ax}=0 m, a=1.2 m (compatible with EC-assisted BKD studies assumptions)

Proposed plan for 2021/2022 activities

Resources proposed for conceptual design study: **0.5 ppy**

- **EC Beam tracing analysis** (GRAY)
  1. Conclude the analysis of the expected power density at specific vessel locations, taking into account the layout and materials therein
- **In vessel ECH sensor study** (ANSYS)
  1. ITER bolometer features and alternatives (pyrodetectors, sniffer probes graphene)
  2. adaptation to JT-60SA (system requirements, materials, thermal & EM simulations, compatibility with operational temperatures, temporal response…)
- **Engineering integration study** (CATIA)
  1. Identification of possible in vessel sensor locations
  2. Requirements for system arrangement and installation
  3. Instrumentation and control
- Prototyping, basic sensor testing, calibration and commissioning plan
- **Report/Deliverables**